# Free space experimental scattering database continuation: experimental set-up and measurement precision



2005 Inverse Problems 21 S117

(http://iopscience.iop.org/0266-5611/21/6/S09)

INSTITUTE OF PHYSICS PUBLISHING INVERSE PROBLEMS

Inverse Problems **21** (2005) S117–S130 doi:10.1088/0266-5611/21/6/S09

# Free space experimental scattering database continuation: experimental set-up and measurement precision

**Jean-Michel Geffrin, Pierre Sabouroux and Christelle Eyraud**

Institut Fresnel UMR CNRSTIC 6133, Université de Provence, Aix-Marseille I, Université Paul Cézanne, Aix-Marseille III, Ecole Généraliste d'Ingénieurs de Marseille, Campus de Saint-Jerôme, case 162, 13397 Marseille Cedex 20, France

E-mail: jean-michel.geffrin@fresnel.fr

Received 8 April 2005, in final form 29 July 2005
Published 25 November 2005
Online at stacks.iop.org/IP/21/S117

**Abstract**

In the present paper, the experimental set-up of Institut Fresnel used to measure the scattered fields of different elongated objects is precisely described. Since the special issue on 'Testing inversion algorithms against experimental data', the modifications of this system, outlined here, have mostly been done to improve the synchronization of the apparatuses and the precision of our measurements. Due to a large number of requests from the inverse problem community, it has been decided to add new measurements to the Institut Fresnel's database. All the new targets presented here are two-dimensional inhomogeneous ones. They are made of different dielectrics or are mixing metal and dielectric parts. Both TE and TM polarizations are measured for each target, from 2 to 10 GHz and even 18 GHz for the most complex target. In the first part of this paper the set-up is described precisely. The second part is devoted to the presentation of the targets. Finally, some TE and TM comparisons of measurements and direct problem simulations are shown to accredit our experimental method and to give an idea of the accuracy of these measurements.

M This article features online multimedia enhancements

(Some figures in this article are in colour only in the electronic version)

## 1. Introduction

One of the main objectives in the first special issue on 'Testing inversion algorithms against experimental data' (Belkebir and Saillard 2001) was to provide to the inverse scattering community real measured fields in an electromagnetic free space configuration. The idea

  

of making scattering measurements in a laboratory-controlled environment to test inversion algorithms was not really new as on three occasions before, in 1996, 1997 and 1999 (McGahan and Kleinman 1996, 1997, 1999), the US Air Force had already provided experimental scattering measurements also known as 'Ipswich data', which were measured in the set-up described in Cote (1992). A few years later, in 2001, our own scattering measurements were a good motivation for a first special section in this same journal. Nowadays, considering

(i) that some recent publications are still exploiting the Ipswich data (Semichaevsky *et al* 2004),
(ii) the still increasing number of citations of articles describing the Institut Fresnel's experimental data (Belkebir and Saillard 2001, Belkebir *et al* 2000),
(iii) the number of groups asking for information about those data,
(iv) the different requests of researchers already involved in the first section (some remarks having even been made during the constitution of the first special issue),
(v) and the demands of people recently using the first part of the Institut Fresnel's database,

it has been decided to add measurements of fields diffracted by other targets to the database with both TE and TM polarization for each target and objects mixing dielectrics or dielectrics and metals.

From our point of view, being involved in the experimental work and not directly in inverse problems, performing bistatic scattering measurements in an anechoic chamber still remains a challenging task for a couple of reasons. First of all, the idea of providing measurements to a large number of people is really stimulating. Second, the different demands have requested us to introduce hardware evolutions and improvements in order to reach rather difficult objectives, such as more complex scattering targets or even three-dimensional (3D) scattering measurements (Geffrin *et al* 2004). As a matter of fact, our chance is also to have access to the anechoic chamber of the Centre Commun de Ressources en Micro-ondes (CCRM) that we can improve and which reveals a really high potential. Another interest in making such measurements is that, at least to our knowledge, there are not many free space electromagnetic scattering measurements available, and despite the Ipswich data, only a few comparable situations have been studied. Maybe some measurements done on tree trunks scattering at EMSL (Fortuny-Guasch 2002) are not very far from what is done here. Some other experiments have also been carried out using a scale factor for studying the optical properties of spheres or sphere aggregates (Gustafson 1996). Even in RCS experiments, bistatic measurements are not really common, but some also have been done at EMSL (Sagues *et al* 2001), at Onera (Gurel *et al* 2003), or at the University of Michigan (Hauck *et al* 1998), but unfortunately it is often not easy to have access to the data due to confidentiality problems.

The specificity of those diffraction measurements requires very careful attention and control of all the experimental parameters, especially because the field of interest is not measured directly but is the result of the subtraction of two measurements. Furthermore, when dealing with targets becoming even more complex, the sensitivity of the system still needs to be increased and the calibration will certainly be a key problem for the next steps of our database. In fact, to get an always better filling of the Ewald's sphere, obtaining the most complete data, including more frequencies and a larger frequency band, many incidence angles and many receiving angles, can become a headache from an experimental point of view. This gives another excellent reason to test algorithms with measured fields, in order to keep in touch 'people developing codes' and 'people connecting cables'. On the occasion of this experimental database constitution, we did already have many exchanges with researchers involved in inversion in our own laboratory and will be really pleased to get contacts with other researchers.

The present paper depicts precisely the experimental set-up used to measure the new scattered fields added to the database. After the description of the principle of those measurements—set-up, equipment and method—the targets under test are described. Comparisons of the experimental scattered fields and the simulated ones in both TE and TM cases are used to estimate the precision of the measurements. Finally, a conclusion is given trying to draw the perspectives of our future work.

## 2. The experimental set-up

### *2.1. Geometrical considerations*

In this database, our aim is to produce measured scattered fields for inversion purposes and to give the opportunity to a large number of scientists to test their algorithms against real measured fields. Therefore all our experiments are carried out in the faradized anechoic chamber of the CCRM (figure 1(a)), a $(14 \times 6.5 \times 6.5)$ m$^3$ room which allows us to simply model all the propagation phenomena as free space ones.

In the present study, as we are measuring the diffraction of elongated objects, we will only use the following arrangement (figure 1(b)). Here the receiver stays in the azimuthal plane $(x0y)$ and is rotated along two-thirds of a circle. In fact, due to the physical existence of the arch, the excursion is restricted to angles going from 60° to 300°. The angular positioning accuracy of this azimuthal arm is 0.01° when moving in a given direction and a bit less, about 0.05°, when reaching the same angular position from the other way (the absolute position being more reproducible when moving in the same direction, clockwise each time for example). Furthermore, instead of moving the source, it has been preferred to keep the antenna at the fixed location ($\theta = 0°$), and to rotate the object itself to obtain different illumination incidences. The rotation stage used for this purpose gives about the same angular accuracy as the azimuthal arm. The arm supporting the object has also been totally re-designed, and is now made of a PA6 tube (diameter = 100 mm and $\varepsilon_r = 2.6$) to allow positioning of rather heavy objects with a higher positioning precision (typically better than 5 mm).

The distance from the transmitter or receiver to the centre of the target has been increased to 1.67 m. In fact this distance has been doubled in order to augment the antenna positioning stability and accuracy. Putting it closer to its fixing device leads also to a better precision when rotating the antenna from TM to TE polarization. Another advantage of putting the antenna a bit further is to limit the antenna to target coupling, the drawback being of course that the object's extremities may have a larger influence on the measured scattered fields. A comparison of 2D simulations and measurements (see further) confirms that our 1.5 m cylinders are tall enough to allow such an assumption.

### *2.2. Measurement considerations*

All the measurements have been done with a vector network analyser (VNA) (Agilent HP 8530) used in a multi-source set-up with two synthesizers and two external mixers, as was done at the beginning of the database. The use of external mixers placed as close as possible to the antennas, as well as the use of an intermediate frequency, leads to a real precision improvement. In fact, as rather long coaxial cables are needed to feed the antennas (typically nine metres, with a typical attenuation of 1.2 dB m$^{-1}$), keeping the high frequency propagation length as short as possible makes our measurements much more stable. The major propagation length in the cables then occurs at a low frequency (20 MHz), avoiding attenuation problems and reducing in the meantime stability difficulties. It can be noticed here

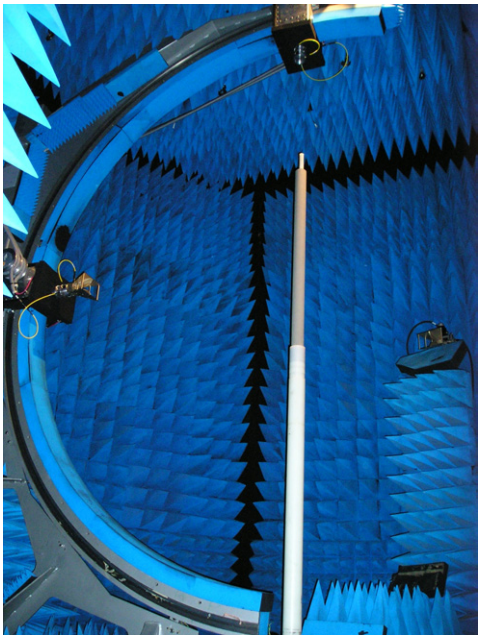

(a) Experimental setup

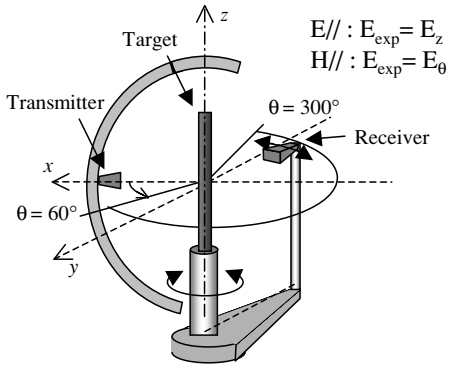


(b) Scheme

**Figure 1.** Free space scattering measurement facility.

that the frequency bandwidth begins now at 2 GHz (instead of 1 GHz) because the technical properties of the mixers were estimated to be not stable enough at this frequency.

The transmitting and receiving antennas are both wide band ridged horn antennas (ARA DRG-118, figure 2) with a frequency range of 1 to 18 GHz (please refer to table 2 for their typical gain and antenna factor). Their polarization is supposed to be linear and their cross polarization level has been measured to be small enough for our study, especially in the object region where the symmetry of the problem makes the cross polarization level obviously small (less than 20 dB below the co-polar level over all the frequency band in the target direction). This last property is important to keep the excitation as close as possible to TM (or E//, the measured field component being $E_z$) or TE (or H//, the measured field component being $E_\theta$). Despite a time of measurement which is almost twice what it could be if we used dual

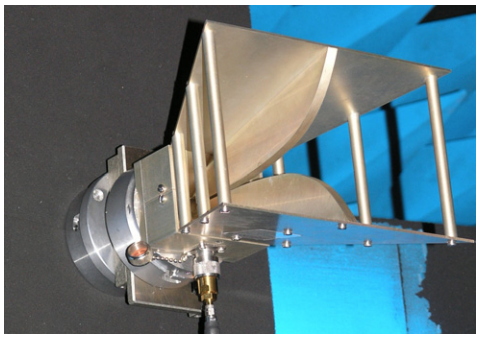

**Figure 2.** ARA-DRG118 ridged horn antenna.

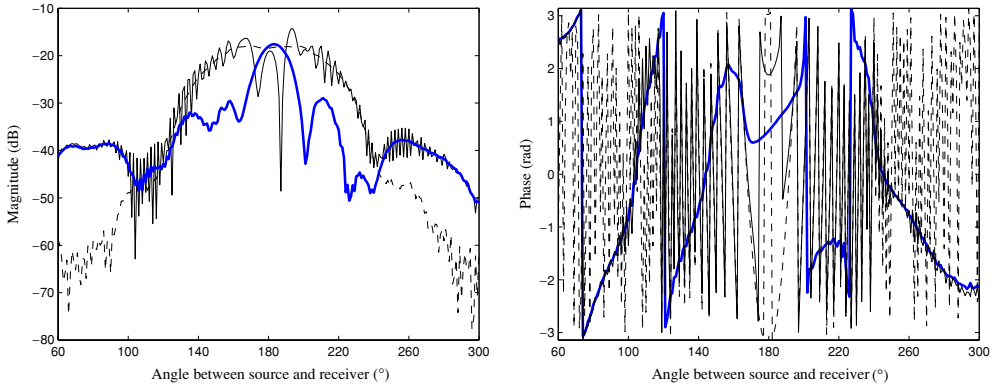


(a) Magnitude (b) Phase

**Figure 3.** Comparison between experimental incident (dotted line), total (thin line) and scattered field (thick line) in TM polarization for the FoamDielExt target ($f = 8$ GHz, $\theta_s = 270°$).

polarization antennas or two sets of two crossed linearly polarized antennas, it has been chosen to change the polarization employing a mechanical rotation of both transmitting and receiving antennas to keep a wide bandwidth and also a good control of the radiation patterns. In practice the measurement of the incident (or total) field is done for every receiver (and source) before rotating the polarization. Evidently the measurements of the two polarization cases are done one just after the other without any movement of the target and both TE and TM cases are measured for each target and at each frequency.

### *2.3. Scattered field measurement protocol*

For any measurements, the same protocol is kept. In such a configuration, the scattered field cannot be measured directly; thus this field is extracted from the subtraction of the total field (the field in the presence of the target) and the incident field (the field measured without any target). The necessity to extract the relevant information from two different measurements makes good stability and a sufficient dynamic really essential. For a given receiver, the scattered field is sometimes more than 10 dB under the actually measured values, i.e. the incident and total field (figure 3).

For each total field, the object is first rotated to its first orientation, the receiver is then moved to its starting position ($\theta = 60°$), there is a short stabilization delay, and the VNA then performs the measurements for each considered frequency. After the end of the VNA

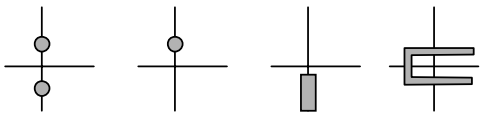

**Figure 4.** First targets: (i) two dielectric circular (Ø = 30 mm, $\epsilon_r = 3$), (ii) one circular dielectric (Ø = 30 mm, $\epsilon_r = 3$), (iii) metallic rectangle (24.5 mm × 12.7 mm) and (iv) U-shaped metal (80 mm × 50 mm).

sweep, the azimuthal arm puts the receiver at its next position and after the stabilization delay the VNA performs the next measurement and so on until the receiver reaches its last position ($\theta = 300^\circ$). After that, one view having been measured, the object is rotated to its next orientation and the receiver scans once again all the possible positions in the azimuthal plane in the other way, starting from 300° and going to 60° to save time. For each incident field measurement the object is removed and a single view is measured clockwise only. Note that measuring the incident field also anticlockwise can reduce our azimuthal arm positioning problem, but as this problem was only identified after the measurements had been provided to the inverse community, we chose to keep the datafiles as they were (including this positioning noise).

All the control software has been totally rewritten in C++, first to remove some remaining bugs, but mainly to achieve a better synchronization of all the involved apparatuses. In this new database the chosen receiver angular step is rather small (one degree) and we are aware that it might have been more interesting to increase the number of sources and reduce the number of receivers for inversion procedures but these small receiver steps are limiting mechanical movements, leading to a shorter total acquisition time. Furthermore, those parameters allow careful control of the experiences and in particular provide us a better understanding of the measurement key features. The number of sources may seem particularly small but as the inversion tests made in our lab are providing correct reconstructions, we only increased it for the two most complex targets.

One of the major criticisms that could be made of this protocol, as the entire measurement of the incident and total fields can take a rather long time (about 30 min for the incident field and $N_s \times 30$ min for the total field, $N_s$ being the number of sources), is that noise and drift errors may highly corrupt the resulting scattered field. Nevertheless, in such a controlled environment and with the rather strong scatterers that were chosen, the stability of the global equipment appears sufficient during the few hours required for each scattered field acquisition. Due to the sensitivity of such measurements to drift errors, one incident field (a single view) has been measured for each total field ($N_s$ views) and each polarization to get the best accuracy. Some work is still being done to try to understand the cause of these problems and part of the issue might be found in small room temperature variations.

## 3. Target description

### *3.1. First targets*

The first edition of our free space scattering database (the files are still freely available on the IoP website http://www.iop.org/EJ/mmedia/0266-5611/17/6/301/) included the measured scattered fields of four homogeneous targets (figure 4), the still growing number of people trying to invert those experimental fields encouraged us to pursue our efforts and to augment the number of available targets.

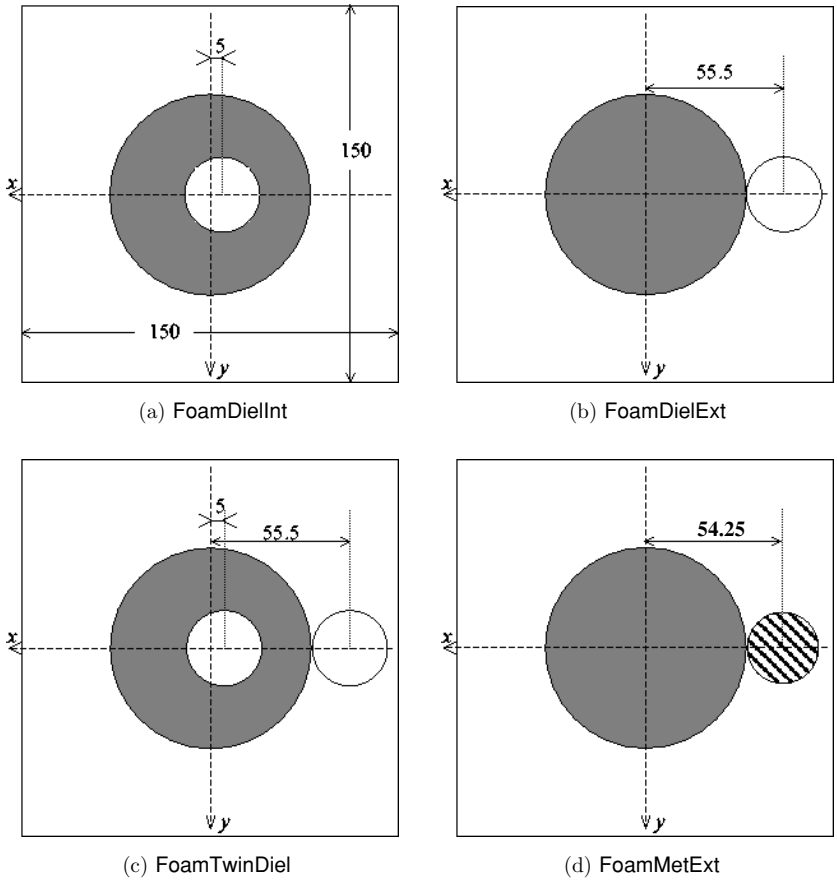


(a) FoamDielInt (b) FoamDielExt

(c) FoamTwinDiel (d) FoamMetExt

**Figure 5.** Description of new targets represented for $\theta_s = 0^\circ$ (dimensions in mm): (white) plastic, (grey) foam, (hatched) copper.

### *3.2. New targets*

The major demands were to furnish both polarizations for each target and also to test non-homogeneous objects. Being now able to present measured scattered fields for four new targets (figure 5) in both TM and TE polarization cases, we decided to propose this new special issue. The retained objects are of two kinds: the first consists of purely dielectric targets, the dielectric cylinders being included one into the other or close together, and the second one is combining a dielectric cylinder and a metallic one. The three different types of cylinders constituting those new targets are the following:

- a foam cylinder (SAITEC SBF 300), diameter = 80 mm, $\varepsilon_r = 1.45 \pm 0.15$,
- a plastic cylinder (berylon), diameter = 31 mm, $\varepsilon_r = 3 \pm 0.3$,
- a copper tube, diameter = 28.5 mm, thickness = 2 mm.

The dielectric constants of these plastics were measured with the VNA and the commercial kit EpsiMu, a coaxial cell associated with a de-embedding technique (Sabouroux and Boschi 2005). The permittivities were found to be almost constant in the 2–18 GHz band and purely real (nearly no losses). All those cylinders are 1.5 m long and were modelled as infinite ones in the following comparisons.

**Table 1.** Summary of the measurement parameters, with $\theta_r = \theta - \theta_s$.

| | Frequencies (GHz) | | | Sources (deg) | | | Receivers (deg) | | |
|---|---|---|---|---|---|---|---|---|---|
| Filename '*.exp' | $N_f$ | $f^{\min}/f^{\max}$ | $\Delta f$ | $N_s$ | $\theta_s^{\min}/\theta_s^{\max}$ | $\Delta\theta_s$ | $N_r$ | $\theta_r^{\min}/\theta_r^{\max}$ | $\Delta\theta_r$ |
| FoamDielIntTM | 9 | 2/10 | 1 | 8 | 0/315 | 45 | 241 | 60/300 | 1 |
| FoamDielIntTE | 9 | 2/10 | 1 | 8 | 0/315 | 45 | 241 | 60/300 | 1 |
| FoamDielExtTM | 9 | 2/10 | 1 | 8 | 0/315 | 45 | 241 | 60/300 | 1 |
| FoamDielExtTE | 9 | 2/10 | 1 | 8 | 0/315 | 45 | 241 | 60/300 | 1 |
| FoamTwinDielTM | 9 | 2/10 | 1 | 18 | 0/340 | 20 | 241 | 60/300 | 1 |
| FoamTwinDielTE | 9 | 2/10 | 1 | 18 | 0/340 | 20 | 241 | 60/300 | 1 |
| FoamMetExtTM | 17 | 2/18 | 1 | 18 | 0/340 | 20 | 241 | 60/300 | 1 |
| FoamMetExtTE | 17 | 2/18 | 1 | 18 | 0/340 | 20 | 241 | 60/300 | 1 |

**Table 2.** Typical antenna factor and gain for the DRG-118/A.

| Frequency (GHz) | Antenna factor (dB $m^{-1}$) | Gain (dBi) |
|---|---|---|
| 1 | 22.93 | 7.3 |
| 2 | 30.15 | 6.1 |
| 3 | 30.67 | 9.1 |
| 4 | 29.97 | 12.3 |
| 5 | 32.81 | 11.4 |
| 6 | 32.99 | 12.8 |
| 7 | 35.33 | 11.8 |
| 8 | 36.79 | 11.5 |
| 9 | 36.21 | 13.1 |
| 10 | 38.03 | 12.2 |
| 12 | 37.81 | 14.0 |
| 14 | 42.35 | 10.8 |
| 16 | 38.51 | 15.8 |
| 18 | 42.54 | 12.8 |

## 4. Useful information to invert those measurements

Below is some useful information which is compulsory for a proper inversion of the measurements:

- The source–object centre and object centre–receiver distances are $d_e = 1.67$ m.
- Every target can be included in a $0.15 \times 0.15\text{m}^2$ square centred at the centre of the receiver circle.
- The receiving positions are taken with a step of $1^\circ$ without any position closer than $60^\circ$ from the source.
- For all the targets except FoamMetExt, the frequencies are taken from 2 to 10 GHz with a step of 1 GHz, FoamMetExt being measured up to 18 GHz.
- The other parameters being more target-dependent, please refer to table 1.

The files layout has been kept identical to that used for the first part of the database, i.e. ASCII files with a 10-line header containing information regarding the target, operating frequencies, polarization, etc:

(i) Integer related to the position of the emitting antenna (source), number 1 means position $(d_e, 0^\circ)$, number 2 corresponds to the position $(d_e, 45^\circ)$ (respectively $(d_e, 20^\circ)$), and so on

upto 8 ($d_e$, 315°) (respectively 18 ($d_e$, 340°)) depending on the target. Here $d_e$ represents the distance between the transmitting antenna and the centre of the experimental set-up.
(ii) Integer related to the position of the receiving antenna. The numbering is the same as for the transmitting antenna but the angular step is 1°.
(iii) Operating frequency in GHz.
(iv) Real part of the total electric field.
(v) Imaginary part of the total electric field.
(vi) Real part of the incident electric field.
(vii) Imaginary part of the incident electric field.

## 5. Comparisons of measured and simulated fields

To estimate the precision of the scattered field measurements gathered in this database and to give an idea of the sensitivity and of the required precision of such measurements, some comparisons of the measured fields and the computed ones will be presented in the following section. All the curves presented here show the linear magnitude and phase of the scattered fields, because, despite the discomfort due to the phase jumps, those parameters were found to be the most representative of any difference or perturbation (the real and imaginary parts of the fields representing more the phase rotation when alternating from positive to negative values than real information).

Note that the only post-processing applied to any of the following results is just one single complex coefficient which multiplies the computed fields to refer energy and phase origin to the measured ones. This calibration factor is simply derived from the ratio of the measured incident field and the simulated one at the receiver located at the opposite of the source ($\theta = 180°$). This really minimal calibration procedure has been used until now because the results are satisfying; but we are aware that some more work needs to be done in this direction and we have already begun to study this problem. Nevertheless a presentation of raw measurements has been preferred here to prove the performances of the set-up itself.

### *5.1. FoamDielExt*

For the sake of comparison, the first chosen target is FoamDielExt, the frequency has been fixed to 8 GHz (figure 6 for experimental scattered fields) (figure 7 for simulated scattered fields). As can be seen, with coloured images, it is not really evident to compare things precisely. This is why we have chosen for the rest of this paper to focus on a given view (270°) plotting amplitude and phase versus receiver angle. In the TM case, the forward problem is solved using the method of moments and domain integral formulations (Harrington 1987). In the TE case, contour integrals are used (Maystre and Vincent 1972) and to avoid any singularity, the two dielectric cylinders are separated by 0.2 mm. The computed field being in fact $H_z$, $E_\theta$ is derived using a finite differentiation of $H_z$ around the receiver circle. When the object is assumed to be at the 'exact' location and the measured permittivities to be the 'exact' ones, some slight differences between simulations and experiments can be observed. Knowing the tolerances of these two parameters, the idea was then to adjust the real position of the target and its dielectric constant in the TM case (figure 8) and then to validate those choices by comparing the TE polarization with the same adjusted parameters (figure 9). As another experiment with the foam cylinder alone did indicate that the value of 1.45 obtained with EpsiMu was correct, we kept this value fixed and corrected the others. The found corrections were to move the centre of the target 2 mm in the $x$ positive direction, 1 mm in the $y$ positive direction and to overestimate the permittivity of the smaller cylinder to 3.3. The coincidence

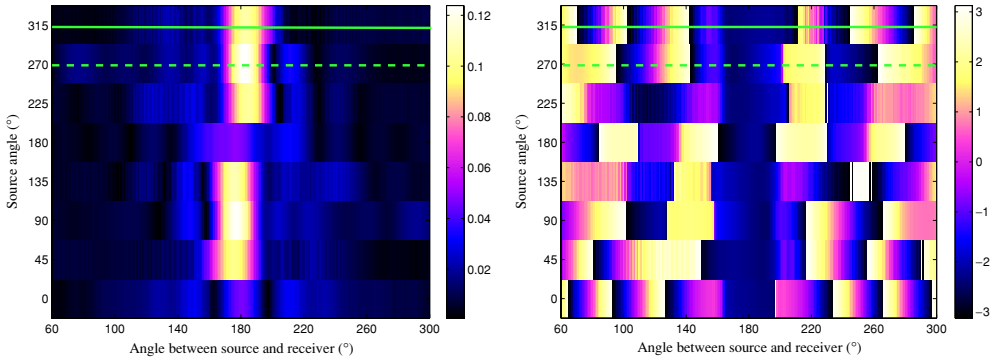


(a) Magnitude (b) Phase

**Figure 6.** Experimental scattered field for the eight sources in TE polarization for the FoamDielExt target ($f = 8$ GHz). The (——) and (- - - -) lines represent fields at $\theta_s = 315°$ and $\theta_s = 270°$ which are plotted in figure 10.

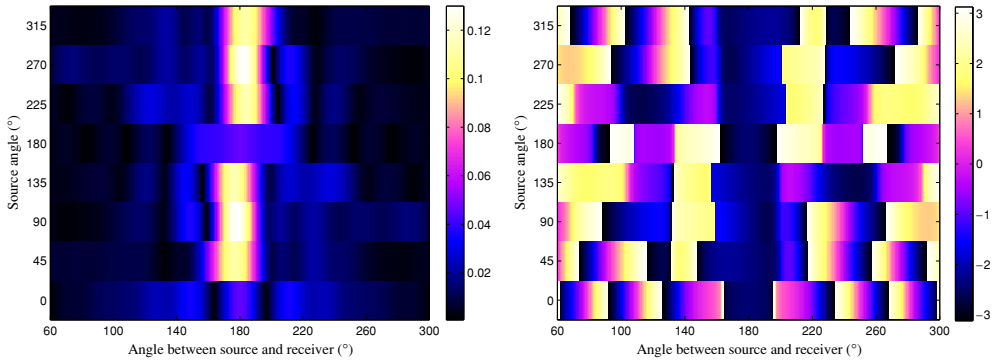


(a) Magnitude (b) Phase

**Figure 7.** Simulated scattered field for the eight sources in TE polarization for the FoamDielExt target ($f = 8$ GHz).

of the measurements and the simulations is thus really improved in the TM case. Indeed the following cost function is then reduced from 0.050 to 0.008,

$$f_c = \frac{\sum_{\text{source}} \sum_{\text{receiver}} \left\| E_d^{\text{simu}} - E_d^{\text{exp}} \right\|^2}{\sum_{\text{source}} \sum_{\text{receiver}} \left\| E_d^{\text{exp}} \right\|^2}, \tag{1}$$

where $E_d^{\text{simu}}$ corresponds to the simulated scattered field and $E_d^{\text{exp}}$ to the experimental one. The correction factors can be considered to be validated by the TE case (the cost function being decreased from 0.041 to 0.017) especially looking at the phase improvement. Furthermore, with respect to the supposed position and dielectric constant accuracy, the magnitude of those correcting factors is totally realistic.

Having a closer look to the results obtained for different incidence angles, it can be seen that one view out of two is more noisy. This can be attributed to the fact that for one view, the total field is measured moving the receiver clockwise, and for the next view anticlockwise. Thus the incident field being measured in the unique clockwise direction, the small positioning difference of the receivers when the total field is measured anticlockwise leads to some oscillations in the scattered field when calculating the subtraction of the total and

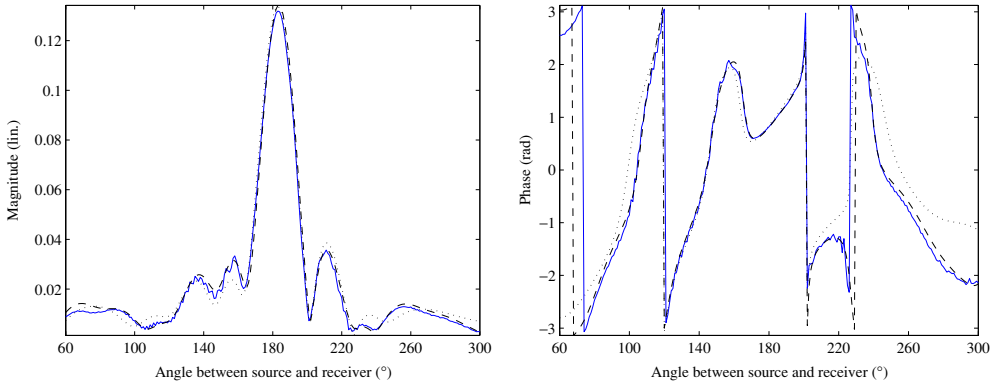


(a) Magnitude (b) Phase

**Figure 8.** Comparison between experimental (——), simulated (· · · · · ·) and simulated with adjusted parameters (- - - -) scattered fields in TM polarization for the FoamDielExt target ($f$ = 8 GHz, $\theta_s = 270°$).

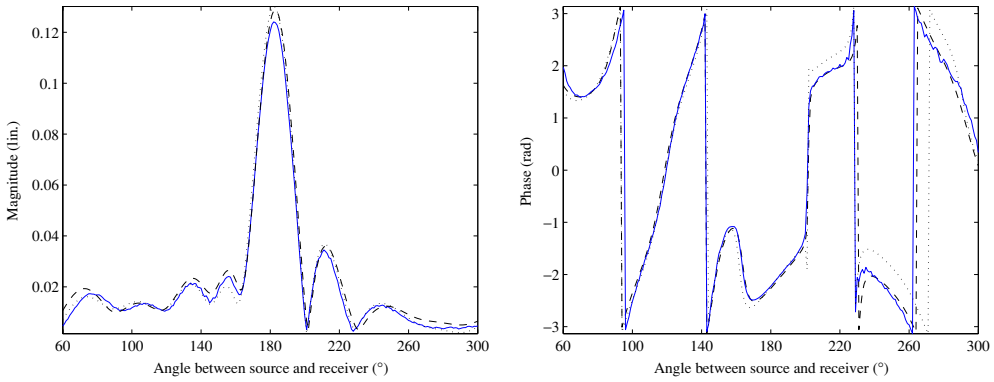


(a) Magnitude (b) Phase

**Figure 9.** Comparison between experimental (——), simulated (· · · · · ·) and simulated with adjusted parameters (- - - -) scattered fields in TE polarization for the FoamDielExt target ($f$ = 8 GHz, $\theta_s = 270°$).

incident fields. This phenomenon is maybe even more visible when overplotting (figure 10) a view $\theta_s = 270°$ (represented in figure 6 by a dashed line where the total field is measured clockwise as incident field, and a view $\theta_s = 315°$ (represented by a full line in figure 6) where the total field is measured anticlockwise.

### *5.2. FoamMetExt*

The FoamMetExt target, which is made of a metallic cylinder and a dielectric one, was supposed to be more complex to invert; thus, we decided to extend the frequency band up to 18 GHz, and as can be seen in raw data at the highest frequency and without any compensating factors for positions and permittivity (figure 11), it can be considered a bit disappointing to have limited other measurements to 10 GHz. In this case, the simulations were performed using the method of moments and assuming the metallic cylinder to be a highly conductive dielectric ($\sigma = 5$ S m$^{-1}$).

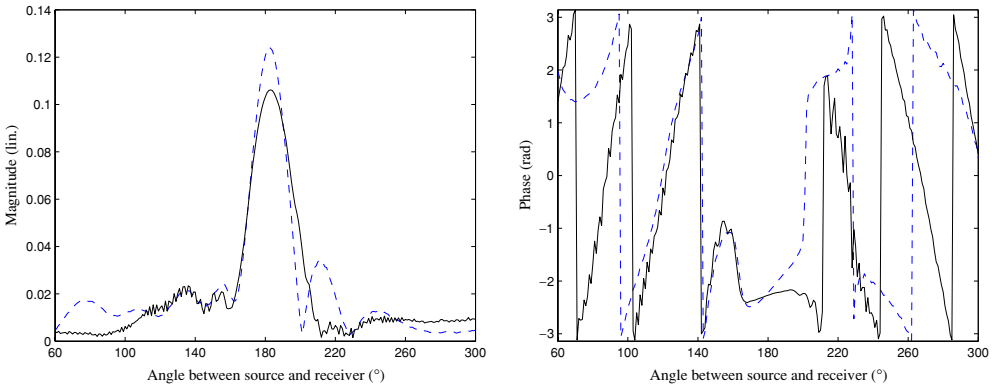


(a) Magnitude (b) Phase

**Figure 10.** Comparison between experimental scattered field in TE polarization for the FoamDielExt target with $\theta_s = 270^\circ$ (- - - -) and $\theta_s = 315^\circ$ (——) ($f = 8$ GHz).

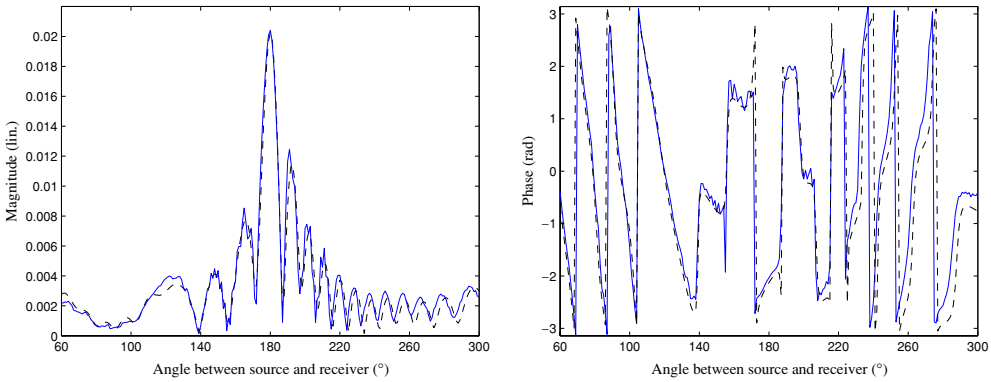


(a) Magnitude (b) Phase

**Figure 11.** Comparison between experimental (——) and simulated (- - - -) scattered field in TM polarization for the FoamMetExt target ($f = 18$ GHz, $\theta_s = 240^\circ$).

## 6. Conclusion and perspectives

The new 2D free space scattering measurements, presented in this paper, will be added to the Institut Fresnel's database. Due to the good agreement between the experiments and TE or TM direct simulations, we are really confident that those data will be useful for inversion purposes. The improvements carried out on the experimental set-up appear to be successful, taking into account that, by augmenting the antennas–object distances, we are now obliged to provide better measurement accuracy and drift control. Despite the remaining errors, the possibility of measuring scattered fields over a rather wide frequency band (2–18 GHz) has also been proven when comparing the FoamMetExt results. As it is not really evident to evaluate how accurate the measurements should be to obtain the best reconstructions, we are very curious about the different inversion results.

Even if the measurements are not perfect yet, the major defaults, mostly attributed to mechanical repositioning errors and to temperature drifts, are under study and some solutions will appear soon (Eyraud *et al* 2005). The careful analysis that was done for this experimental

campaign has provided us a deeper understanding of the process. Thus we can claim that we would get better measurements if we were performing the same experiments today. Scattering by even more complex 2D targets, if there is any interest, could then be tackled. In the meanwhile, thanks to the wide frequency range, some preliminary studies have also been carried out on pulse synthesis with 2D targets and this work might also be extended (Dubois *et al* 2005).

Finally, as has already been mentioned previously, some work on 3D scattering measurements has already been done. The addition of a second waggon on the arch will largely augment the degrees of freedom for measurements all around the target. Some comparisons of measurements performed in a meridian plane or in an equatorial plane (Geffrin *et al* 2004) have already proven the potentials of our system, but due to the much lower level of the scattered field and to the increased number of mechanical positioning devices involved in those measurements, all the previous difficulties are emphasized. Nevertheless, we hope to be able to provide soon 3D scattering measurements for an eventual continuation of the database.

As for the experimental work itself, the main directions of our future studies will certainly concern the calibration of our system, appearing essential if cross polarization measurements are required, as was pointed out by our first 3D experiments. Some better knowledge of the antenna radiation characteristics might also be of great interest, especially concerning the incident field in the object region. Some probe compensation might also draw your attention even if we forgot those considerations previously, being ourselves surprised with the accuracy of the rather simple propagation models that have been used until now.

## Acknowledgment

We would like to thank Amelie Litman and Patrick Vincent for their patient help in our direct problem comparisons.

## References

Belkebir K, Bonnard S, Pezin F, Sabouroux P and Saillard M 2000 Validation of 2D inverse scattering algorithms from multifrequency experimental data *J. Electromagn. Waves Appl.* **14** 1637–67

Belkebir K and Saillard M 2001 Guest Editors' introduction. Special section: Testing inversion algorithms against experimental data *Inverse Problems* **17** 1565–71

Cote M G 1992 Automated swept-angle bistatic scattering measurement using continuous wave radar *IEEE Trans. Instrum. Meas.* **41** 185–92

Dubois A, Belkebir K and Saillard M 2005 Iterative solution of the inverse scattering problem from transient scattered field *IEEE AP-S Int. Symp. UNC–URSI National Radio Science Meeting (Washington, DC, USA)*

Eyraud C, Geffrin J and Sabouroux P 2005 On the accuracy of scattering measurements in free space: random and systematic errors *11th Int. Symp. ANTEM (Saint Malo, France)* pp 352–3

Fortuny-Guasch J 2002 A novel 3D subsurface radar imaging technique *IEEE Trans. Geosci. Remote Sens.* **40** 443–52

Geffrin J, Eyraud C, Sabouroux P and Tortel H 2004 3D scattering measurements, validation with canonical targets *Mediterranean Microwave Symp. (Marseille, France)*

Gurel L, Bagci H, Castelli J C, Cheraly A and Tardivel F 2003 Validation through comparison: measurement and calculation of the bistatic radar cross section (BRCS) of a stealth target *Radio Sci.* **38** 12.1–12.10

Gustafson B A S 1996 Microwave analog to light scattering measurements: a modern implementation of proven method to achieve precise control *J. Quant. Spectrosc. Radiat. Transfer* **55** 663–72

Harrington R 1987 The method of moments in electromagnetics *J. Electromagn. Waves Appl.* **1** 181–200

Hauck B, Ulaby F and DeRoo R 1998 Polarimetric bistatic measurement facility for point and distributed targets *IEEE Antennas Propagat. Mag.* **40** 31–40

Maystre D and Vincent P 1972 Diffraction d'une onde électromagnétique plane par un objet cylindrique non infiniment conducteur de section arbitraire *Opt. Commun.* **5** 327–30

McGahan R and Kleinman R 1996 Special session on image reconstruction using real data *IEEE Antennas Propag. Mag.* **38** 39–40

McGahan R and Kleinman R 1997 Second annual special session on image renconstruction using real data *IEEE Antennas Propag. Mag.* **39** 7–9

McGahan R and Kleinman R 1999 Third annual special session on image renconstruction using real data, Part 1 *IEEE Antennas Propag. Mag.* **41** 34–6

Sabouroux P and Boschi P 2005 EpsiMu: a new microwave materials measurements kit *European Test and Telemetry Conf. (Toulouse, France)*

Sagues L, Lopez-Sanchez J M, Fortuny J, Fabregas X, Broquetas A and Sieber A 2001 Polarimetric radar interferometry for improved mine detection and surface clutter rejection *IEEE Trans. Geosci. Remote Sens.* **39** 1271–8

Semichaevsky A, Testorf M, McGahan R and Fiddy M 2004 Unsupervised constrained radar imaging resolution targets *Waves Random Media* **14** 415–34